# Genetic disruption of ankyrin-G in adult mouse forebrain causes cortical synapse alteration and behavior reminiscent of bipolar disorder

Shanshan Zhu[a,b], Zachary A. Cordner[b], Jiali Xiong[a,b], Chi-Tso Chiu[c], Arabiye Artola[a,b], Yanning Zuo[a,b], Andrew D. Nelson[d], Tae-Yeon Kim[a,b], Natalya Zaika[a,b], Brian M. Woolums[e], Evan J. Hess[a,b], Xiaofang Wang[a,b], De-Maw Chuang[c], Mikhail M. Pletnikov[a,b,f,g,h], Paul M. Jenkins[d,i], Kellie L. Tamashiro[b], and Christopher A. Ross[a,b,e,f,j,1]

[a]Division of Neurobiology, Department of Psychiatry, Johns Hopkins University School of Medicine (JHU SOM), Baltimore, MD 21287; [b]Department of Psychiatry, JHU SOM, Baltimore, MD 21287; [c]Section on Molecular Neurobiology, National Institute of Mental Health, National Institutes of Health, Bethesda, MD 20892; [d]Department of Pharmacology, University of Michigan Medical School, Ann Arbor, MI 48109; [e]Department of Pharmacology and Molecular Sciences, JHU SOM, Baltimore, MD 21287; [f]The Solomon H. Snyder Department of Neuroscience, JHU SOM, Baltimore, MD 21287; [g]Department of Molecular and Comparative Pathobiology, JHU SOM, Baltimore, MD 21287; [h]W. Harry Feinstone Department of Molecular Microbiology and Immunology, JHU Bloomberg School of Public Health, Baltimore, MD 21287; [i]Department of Psychiatry, University of Michigan Medical School, Ann Arbor, MI 48109; and [j]Department of Neurology, JHU SOM, Baltimore, MD 21287

Genome-wide association studies have implicated the *ANK3* locus in bipolar disorder, a major human psychotic illness. *ANK3* encodes ankyrin-G, which organizes the neuronal axon initial segment (AIS). We generated a mouse model with conditional disruption of *ANK3* in pyramidal neurons of the adult forebrain (Ank-G cKO). This resulted in the expected loss of pyramidal neuron AIS voltage-gated sodium and potassium channels. There was also dramatic loss of markers of afferent GABAergic cartridge synapses, resembling the cortical micro-circuitry changes in brains from psychotic patients, and suggesting disinhibition. Expression of c-fos was increased in cortical pyramidal neurons, consistent with increased neuronal activity due to disinhibition. The mice showed robust behavioral phenotypes reminiscent of aspects of human mania, ameliorated by antimania drugs lithium and valproate. Repeated social defeat stress resulted in repeated episodes of dramatic behavioral changes from hyperactivity to "depression-like" behavior, suggestive of some aspects of human bipolar disorder. Overall, we suggest that this Ank-G cKO mouse model recapitulates some of the core features of human bipolar disorder and indicates that cortical microcircuitry alterations during adulthood may be involved in pathogenesis. The model may be useful for studying disease pathophysiology and for developing experimental therapeutics.

*ANK3* | mania | axon initial segment | chandelier synapse | lithium

**B**ipolar disorder and schizophrenia are major psychiatric disorders. Bipolar patients experience both mania, with elevated mood and activity, and depression (often triggered by stress), with low mood and activity. Bipolar disorder is often uniquely responsive to lithium (Li). Many loci have been identified by genome-wide association studies (GWASs) for schizophrenia (1). By contrast, fewer loci with genome-wide significance have been identified for bipolar disorder (2), with some overlap, suggesting some shared mechanisms.

In a recent large GWAS of bipolar disorder (3), the most significant signal was detected at the *ANK3* locus. This finding has been replicated in many (if not all) GWASs of bipolar disorder (3–5). The *ANK3* locus is also found to be associated, to a lesser extent, with schizophrenia (6, 7).

The *ANK3* gene encodes ankyrin-G, a large scaffold protein highly expressed in neurons in the brain (8). Three main brain-specific splice variants encode 190, 270, and 480 kDa polypeptides. The 480-kDa peptide is the major isoform responsible for organization of the components of the axon initial segment (AIS), including the clustering of voltage-gated sodium and potassium channels important for generation of the action potential (9, 10). The 190-kDa isoform is present at dendritic spines (11, 12). Many of the risk alleles for *ANK3* are in the five-prime upstream region, suggestive of changes of expression (13, 14). Ankyrin-G protein expression was reduced in pyramidal AISs in

superficial layers of schizophrenia cortex (15). These data suggest that *ANK3* risk alleles can cause ankyrin-G loss of function.

In cortex, the AISs of pyramidal neurons are innervated by inhibitory synapses from chandelier cells, fast spiking interneurons, whose synapses form GAT-1 and GAD67 positive cartridge-like structures around ankyrin-G positive AISs (16). Thus, the AIS is an important site for cortical microcircuit regulation (9), disruptions of which may contribute to schizophrenia and bipolar disorder (17). Both mRNA and protein level of GAT-1 and GAD67 are decreased in schizophrenia patients' postmortem brains (18, 19). It is difficult to study the effects of decreased ankyrin-G in humans, but a genetic mouse model might elucidate behavioral and cellular effects of decreased ankyrin-G expression in the forebrain.

A previous study described viral vector-mediated knockdown of ankyrin-G in hippocampus and heterozygous deletion of a brain-specific isoform highly expressed in cerebellum. Both models yielded intriguing behavioral changes (20), but the behavioral changes were subtle and only partly reflect bipolar disorder.

In this study, we have generated a mouse model with homozygous deletion of all major isoforms of ankyrin-G in pyramidal neurons of the adult forebrain. We found a robust behavioral

## Significance

The *ANK3* gene locus has been repeatedly shown to confer risk for bipolar disorder in genome-wide association studies. We generated a mouse model with conditional disruption of *ANK3* gene in neurons in adult forebrain (Ank-G cKO). The mice showed robust behavioral phenotypes reminiscent of aspects of human mania, ameliorated by antimania drugs. Repeated stress resulted in dramatic behavioral changes between "mania-like" and "depression-like" status, reminiscent of human bipolar disorder. Histological studies imply that cortical microcircuitry alterations are involved in pathogenesis. Overall, we suggest that this Ank-G cKO mouse model recapitulates core features of human bipolar disorder, and may be useful for studying disease pathophysiology and for developing experimental therapeutics.

NEUROSCIENCE

phenotype reminiscent of some aspects of human mania. Furthermore, we observed dramatic loss of inhibitory cartridge synapses and elevated c-fos expression in relevant brain regions. The "manic-like" behaviors were substantially ameliorated by classic antimania drugs lithium and valproic acid (VPA). After social defeat stress, there was a switch to "depression-like" behavior, with alternation between mania-like and depression-like behavior upon repeated stress. We propose that our genetic mouse model recapitulates some of the key features of human bipolar disorder.

## Materials and Methods

**Animals.** All experiments were conducted following protocols approved by the Institutional Animal Care and Use Committee at JHU SOM. Ankyrin-G floxed mice (*Ank3flox/flox*) with loxP sites flanking exons 22 and 23 of the *Ank3* gene (21) were crossed with *Camk2a*-Cre mice (JAX) for forebrain-specific homozygous deletion of ankyrin-G (*Camk2a*-Cre; *Ank3flox/flox*) (named Ank-G cKO), in which exons 22 and 23 of both alleles of the *Ank3* gene were excised. Littermates that did not express Cre were used as controls (*Ank3flox/flox*). All analysis was performed using mice 3.5–7 mo old.

**Western Blots.** Western blots were performed essentially as described (10); details can be found in *SI Materials and Methods*.

**Behavior Tests.** Behavioral tests are described in *SI Materials and Methods*. Mice were housed by sex with three to four mice/cage. Except for a 24-h open field test, all behavioral tests were done during the light (sleep) phase of mice. Major experiments were repeated using more than two cohorts of mice.

**Drug Treatment.** Lithium and valproate were given via chow food for 3 wk to achieve therapeutic levels, and behavior tests were carried out the next day after the end of the drug treatments.
*Lithium.* Mice were fed with 0.2% lithium carbonate chow (Harlan) for 1 wk followed by 2 wk of 0.4% lithium carbonate chow, supplemented with a bottle of saline (22). The serum lithium concentration was $0.825 \pm 0.082$ mEq/L.
*Valproic acid.* Mice were fed with chow containing 1.7% sodium valproic acid for 3 wk. The serum VPA concentration was $52.8 \pm 6.9$ mg/L.
*Methylphenidate.* Twenty-five minutes before open field test, mice were treated with methylphenidate (dissolved in saline) via i.p. injection at 10 mg/kg or 30 mg/kg body weight. More details can be found in *SI Materials and Methods*.

**Brain Section Preparation, Immune Labeling, and Image Quantification.** Perfusion, sectioning and immunolabeling were performed using standard techniques described in *SI Materials and Methods*. Antibodies are listed in Table S1. Immunofluorescence images were acquired using confocal microscopy; see *SI Materials and Methods*. In each experiment, we used four to six mice per group and two to seven sections per mouse for quantification and statistical analysis.

**Social Defeat Stress.** Mice were repeatedly stressed for 14 d using standard protocols (23) as described in *SI Materials and Methods*. Behavioral tests and adrenal gland weighing were done within 1 wk after stress.

**Statistical Analysis.** Statistical analyses were performed using SigmaStat (Systat Software, Inc.) and Statistica 7 (StatSoft, Inc.); see *SI Materials and Methods*.

## Results

**Generation of Forebrain-Specific Ankyrin-G KO Mice.** We generated a conditional *Ank3* KO mouse (Ank-G cKO) with homozygous loss of ankyrin-G expression in forebrain (e.g., cortex, hippocampus, and striatum) pyramidal neurons starting from adolescence. Mice were studied at 3 mo of age or older, when there were consistent changes in ankyrin-G expression and behavior. Using immunofluorescent labeling, we found that more than 60% of neurons in the cortex lost ankyrin-G at AISs (Fig. 1*A* and Fig. S1). Ankyrin-G expression was lost in at least 70% of pyramidal neurons marked by CaMKII(+) labeling (Fig. S1 *F* and *G*), but not in parvalbumin(+) fast spiking interneurons (Fig. S1 *J* and *K*). Western blots demonstrated a decrease of all three major isoforms of ankyrin-G expression (190, 270, and 480 kDa) in forebrain regions (cortex and hippocampus) of Ank-G cKO mice (Fig. S2).

## Ank-G cKO Mouse Cortical Pyramidal Neurons Lose Ion Channel Expression at the AIS and Show Dramatic Decrease of Markers of GABAergic Cartridge Synapses. In Ank-G cKO mouse forebrain (including cortex and hippocampus), we found a substantial loss of sodium and potassium channels at AISs (Fig. S3 *E* and *F*),
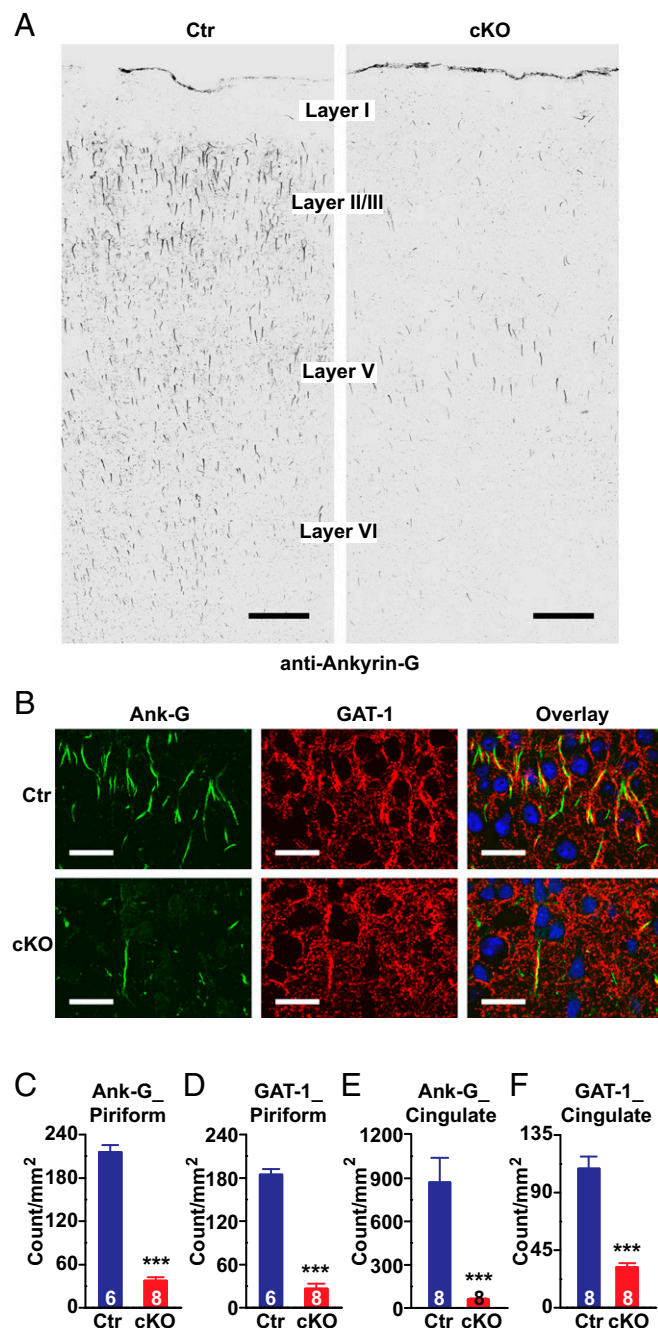


**Fig. 1.** Genetic deletion of ankyrin-G in AISs of pyramidal neurons of mouse forebrain, and alteration of presynaptic GABA markers. (*A*) Confocal images of mouse motor cortex immunolabeled with anti–ankyrin-G antibody showing loss of ankyrin-G at AIS in Ank-G cKO mouse. (Scale bar: 100 μm.) (*B*) Confocal images of mouse piriform cortex labeled with anti–ankyrin-G (green) and anti–GAT-1 (red) antibodies in wild-type (*Top*) and Ank-G cKO (*Bottom*) mice. (Scale bars: 30 μm.) The nuclei are labeled with DAPI (blue). (*C*–*F*) Quantification of ankyrin-G (*C* and *E*) and GAT-1 (*D* and *F*) at AIS in mouse piriform cortex (*C* and *D*) and cingulate cortex (*E* and *F*). Bar graphs represent mean ± SEM; ***$P < 0.001$, Student $t$ test. The number of animals per group is indicated at the bottom of each bar graph.

consistent with prior primary results (10, 24). In cortex, chandelier inhibitory neurons normally form synapses in cartridge-like structures innervating pyramidal neuron AISs (16). Cartridge-like structures in mouse are most evident in the piriform cortex, as shown by labeling with anti-GAD67 and anti–GAT-1 antibodies (25); the GAT-1 cartridges are also present in cingulate cortex (26). We examined GAT-1–labeled cartridges in piriform and cingulate cortex, and GAD67-labeled cartridges in piriform cortex. Fig. S3B shows an example of GAD67-labeled cartridges presynaptic to ankyrin-G AIS in the piriform cortex. In piriform cortex of cKO mice, there was a dramatic reduction in the number of GAT-1 (Fig. 1 B and D) and GAD67 positive (Fig. S2 B and C) cartridge synaptic markers. We also observed significantly decreased GAT-1 cartridges in cingulate cortex—a brain region involved in emotion processing (Fig. 1 E and F). Ankyrin-G expression is also greatly reduced in these brain regions (Fig. 1 B, C, and E and Fig. S3 B and C).

**Ank-G cKO Mice Display Mania-Like Behaviors.** Overall, male and female mice show very similar behavioral phenotypes; therefore, unless mentioned, all of the behavioral results shown in Fig. 2 are from male mice, in comparison with littermate controls.
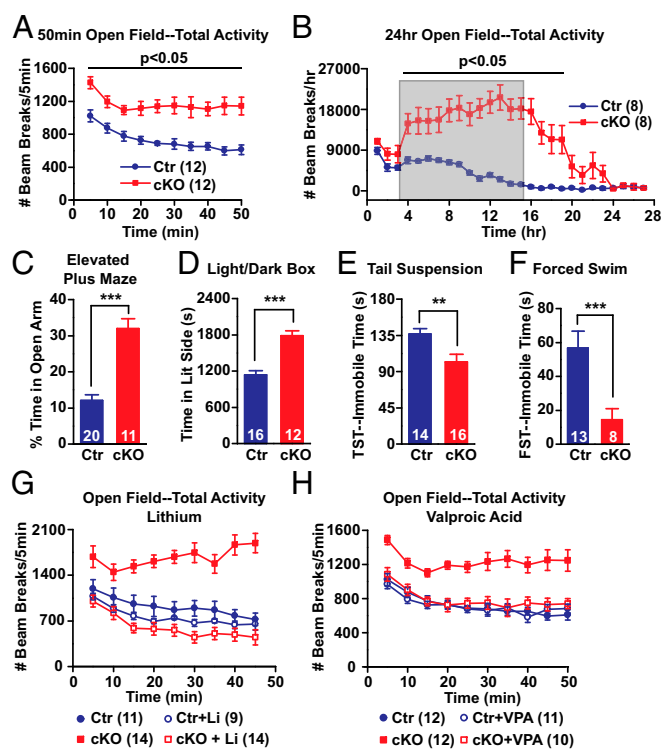


**Fig. 2.** Behavioral characterization and drug rescue. (A and B) Open field test for locomotor activity: (A) 50 min and (B) 24 h. Number of infrared beam breaks every 5 min (A) or every hour (B). Shaded area in B indicates the typical active time of control mice (9 PM–9 AM). Two-way repeated measurement of ANOVA followed by post hoc t test are shown. (C–F) Tests for anxiety and depression-like behavior. (C) Elevated plus maze: percent of time mice spend in the open arm during 6 min. (D) Light/dark box: the time(s) that mice spent in light box. (E and F) The total immobile time(s) of mice in tail suspension test (E) and forced swim test (F). Bar graphs represent mean ± SEM; ***$P <$ 0.001, **$P <$ 0.01, Student t test. (G and H) Open field test of lithium-treated (G) and VPA-treated (H) mice. Number of infrared beam breaks every 5 min. Li: Mice were fed with 0.2% lithium carbonate chow for 1 wk, followed by 0.4% for 2 wk. VPA: 1.7% sodium valproate chow for 3 wk. Factorial repeated measurement of ANOVA followed by post hoc t test are shown. We detected significant gene × drug interactions in G [$F_{(1, 44)} =$ 20.77, $P <$ 0.001] and H [$F_{(1, 41)} =$ 10.90, $P =$ 0.002]. The number of animals per group is indicated in figure legend or at the bottom of each bar graph.

We did not observe any differences between Ank-G cKOs and their littermate controls in appearance, grooming behavior, or body weight gain, up to at least 7 mo of age. However, Ank-G cKO mice were hyperactive in a 50-min open field test (Fig. 2A and Fig. S4A). In a 24-h open field test (lights on at 9 AM, off at 9 AM), cKO mice showed dramatic hyperactivity during the dark between 9 AM and 9 AM, the "active" period for mice (Fig. 2B and Fig. S4D), which continued for several additional hours after entering the light or "inactive" period. In both tests, the Ank-G cKO mice also spent significantly more time exploring the center zone of the box than control (Fig. S4 B, C, E, and F), implying elevated exploratory behavior and decreased "anxiety." The hyperactivity is not caused by novel environment, because in a 3-d open field test, cKO mice, after habituation on the first day, continued being hyperactive on second and third days (Fig. S4 P and Q).

To further examine the anxiety and exploratory phenotype, we assessed behavior in the elevated plus maze (EPM) and light/dark box tests. In the elevated plus maze, the percentages of time and distance Ank-G cKO mice spent/traveled in the open arm were about threefold higher than those of control mice (Fig. 2C and Fig. S4G). In the light/dark box test, Ank-G cKO mice remained in the lit compartment significantly longer than controls (Fig. 2D). cKO mice traveled longer distances and at a faster speed in the elevated plus maze test and displayed a greater number of transitions between the two boxes in the light/dark box test (Fig. S4 H–J). Thus, Ank-G cKO mice displayed increased exploratory and reduced anxiety-like behaviors compared with littermate controls.

To evaluate depression-like behavior, we performed the tail suspension test and forced swim test (FST). In both tests, the time mice spent immobile was shorter in cKO mice compared with controls (Fig. 2 E and F), indicating decreased depression-like behavior.

Cognitive decline is one of the core features of patients with schizophrenia, and may be present, but is usually less prominent, in bipolar disorder (27). We performed Y maze tests (spatial learning and memory), and 1-h and 24-h novel object recognition tests (short- and long-term visual memory). Ank-G cKO mice showed some deficit in Y maze, but not in the novel object recognition test (Fig. S4 K–O).

Prepulse inhibition (PPI) is a standard measure of sensorimotor gating. PPI deficit is thought to be characteristic of schizophrenia, but less consistently observed in bipolar patients (28). Animal models of schizophrenia typically show deficits in PPI (29). Ank-G cKO mice demonstrated no obvious deficit in PPI (Fig. S5 A and B).

Hyperactivity is also seen with attention deficit hyperactivity disorder (ADHD) (30). Methylphenidate is used to decrease ADHD patients' hyperactivity, but it increases the activity of individuals without ADHD (30). Methylphenidate at two different doses made cKO mice even more active (Fig. S5 C–F), unlike what would be expected in a mouse model of ADHD.

**Mania-Like Behavior in the Ank-G cKO Mice Is Reversed with Clinically Effective Antimania Drugs.** We tested whether Li and VPA, drugs effective for human mania, altered the behaviors, such as hyperactivity (open field) or elevated exploration/decreased anxiety (elevated plus maze) of Ank-G cKO animals. We fed mice with chow containing $Li_2CO_3$ chronically, achieving blood lithium concentration within the human therapeutic range. Lithium had little effect on the behavior of control mice in the open field test, but reduced Ank-G cKO mice locomotor activity to levels comparable to that of control (Fig. 2G and Fig. S5G). The central activity of Ank-G cKO mice was also decreased upon lithium treatment (Fig. S5 H and I). We also fed mice with VPA containing chow chronically. The open field test showed that the effects of VPA on control and cKO mice are similar to lithium (Fig. 2H and Fig. S5 J–L). In the elevated plus maze test, VPA significantly reduced the elevated exploratory behavior of cKO mice to the level comparable to control, with little effect on control mice (Fig. S5 M–P).

**Ank-G cKO Mice Pyramidal Neurons Exhibit Increased c-fos Expression.** We reasoned that the increased locomotor activity of Ank-G cKO mice might involve increased neuronal activity of pyramidal neurons
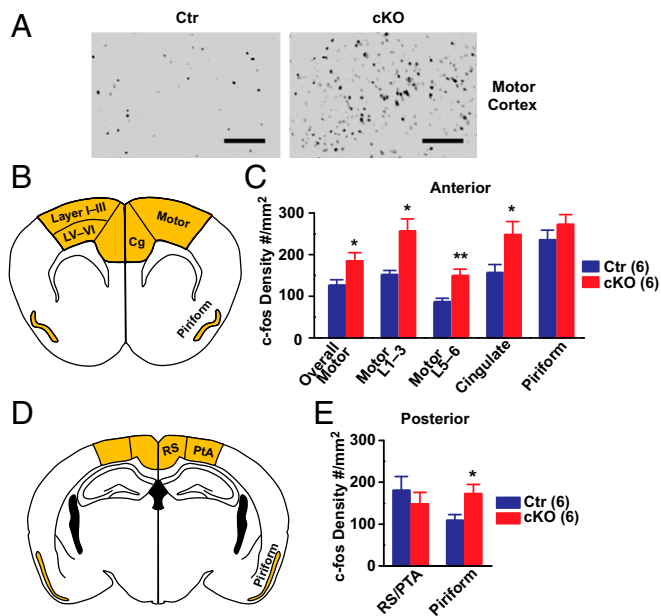
NEUROSCIENCE

**Fig. 3.** Ank-G cKO mice displayed elevated c-fos labeling, indicating increased cortical neuronal activity. (A) Representative pictures of the DAB labeling on mouse motor cortex with anti–c-fos antibody. (Left) Control; (Right) Ank-G cKO. (Scale bar: 100 μm.) (B and C) Schematic illustration and quantification of c-fos expression at indicated brain regions in anterior cortex (Bregma 1.42 mm) of Ank-G cKO and control mice. Brain regions used for quantification are highlighted in B, including motor, cingulate, and piriform cortex. Motor cortex is further divided into layers I–III, and layers V and VI for quantification. (D and E) Schematic illustration and quantification of c-fos expression in posterior cortex (Bregma −2.06 mm). Brain regions used for quantification are highlighted in D, including RS/PTA and piriform cortex. RS/PTA is the region comparable to anterior motor + cingulate cortex, i.e., retrosplenial cortex (RS) and parietal association cortex (PTA). Bar graphs represent mean ± SEM; **$P < 0.01$, *$P < 0.05$, Student $t$ test. The number of animals in each group is indicated in parentheses.

in the motor cortex, and the elevated emotion-related behavior (altered anxiety, exploration, and depression-like behavior) might involve altered activity in the cingulate cortex. To test this hypothesis, we placed control or Ank-G cKO mice into an activity chamber for 25 min and compared the expression of c-fos, a marker for neuronal activity, between Ank-G cKO and control mice. We also assessed c-fos in posterior piriform cortex, where GABA synapse loss was detected in Ank-G cKO mice.

We first examined c-fos expression via 3,3′-diaminobenzidine (DAB) labeling (Fig. 3A). We chose the retrosplenial dysgranular cortex (RSD), medial parietal association cortex (MPtA), and lateral parietal association cortex (LPtA) together labeled as RS/PTA, and the anterior piriform cortex (where ankyrin-G levels were not changed) as comparison regions. As shown in Fig. 3 B–E, compared with control, cKO mice had significantly increased c-fos labeling, in motor, cingulate (B and C) [compared with comparison region RS/PTA (D and E) on posterior section] and posterior piriform cortex (D and E) [compared with anterior piriform cortex (B and C)], but not in comparison regions. We further divided motor cortex into layers I–III (intracortical association) and layer V and VI (projection) (B and C). Both regions showed elevated c-fos activity in Ank-G cKO mice compared with controls. We further examined cell types with increased c-fos expression and found the elevated c-fos expression was only present in CaMKII positive excitatory pyramidal neurons, not in parvalbumin positive inhibitory neurons (Fig. S6 B and D). The overall number of CaMKII positive and parvalbumin positive neurons remained the same between control and cKO mice (Fig. S6 E and F).

## Social Defeat Stress Induces Depressive-Like Behaviors in Ank-G cKO Mice.

The hallmark of bipolar disorder in human is the presence of episodes of both mania and depression, and stress is known to precipitate depression (31). Prior studies in rodents have demonstrated that exposure to social defeat stress results in depression-like behavior (32). After 14 d of chronic social defeat stress (23, 32), Ank-G cKO mice displayed significantly reduced motor activity in open field test (Fig. 4A and Fig. S7A) and decreased exploratory behavior in EPM (Fig. 4B). Both measures were reduced to levels comparable to those of socially defeated control mice, which is lower than nonstressed control. Similarly, in the FST for depression-like behavior, after stress, Ank-G KO mice displayed a large increase in immobile time vs. a relatively small increase for controls (Fig. 4C). Ank-G cKO mice were more susceptible to stress than control: the gene × stress interactions are significant in open field and EPM tests. Upon stress, there are greater fold changes for cKO than control [EPM (B): 9.8-fold vs. 2.7-fold]. In addition, Ank-G cKO mice exhibited submissive behavior and adrenal hypertrophy after social defeat stress, indistinguishable from stressed control mice (Fig. S7B).

When allowed to recover and then reexposed to social defeat stress, cKO mice but not controls, first returned to the hyperactivity, and then again displayed hypoactivity, as indicated by total activity in the open field test (Fig. 4D). Elevated plus maze or forced swim test cannot be readily repeated in the same mice; however, open field central activity also showed switching between mania-like and depression-like behavior (Fig. 4E).
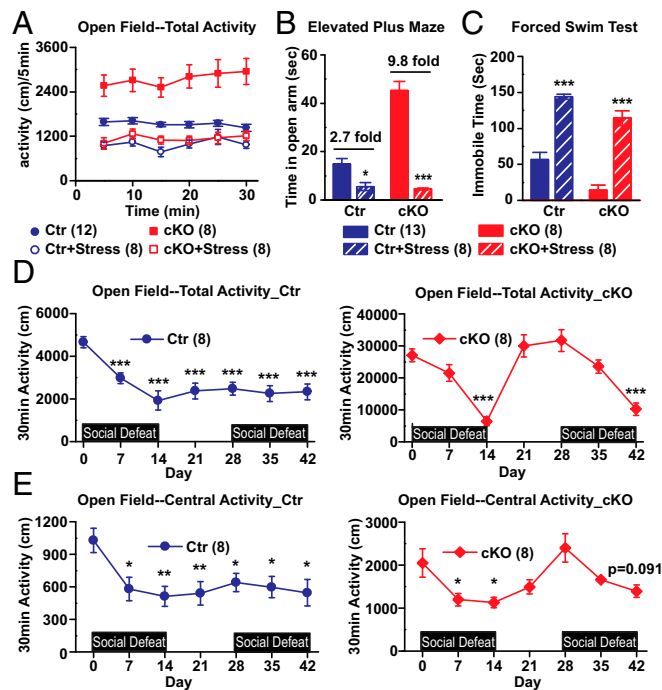


**Fig. 4.** Ank-G cKO mice displayed depression-like behavior upon chronic social defeat stress. (A) Thirty-minute open field test. Distance traveled (in centimeters) every 5 min. Factorial repeated measurement of ANOVA followed by Tukey post hoc $t$ test. (B) The time(s) mice spent in open arm of the elevated plus maze. (C) The immobile time(s) of mice in forced swim test. Two-way ANOVA followed by Tukey post hoc $t$ test. Bar graphs represent mean ± SEM; ***$P < 0.001$, *$P < 0.05$, compared with nonstressed control or cKO. (D and E) Thirty-minute open field test throughout two rounds of social defeat stress. Total distance traveled (in centimeters) in the whole box area (D) or in central area (E) alone at different time point. Each time point was compared with baseline using Student $t$ test. ***$P < 0.001$. The number of animals in each group is indicated in parentheses. We detected significant gene × environment interactions in A [$F_{(1, 32)} = 12.14$, $P = 0.0015$] and B [$F_{(1, 33)} = 42.67$, $P < 0.001$] but not C [$F_{(1, 33)} = 0.51$, $P = 0.480$].

## Discussion

Although there have been many attempts to develop genetic mouse models of schizophrenia (33), there have been relatively few reports of genetic mouse models of bipolar disorder, especially based on loci with replicated genome-wide significance in human genetic studies (34). In our conditional KO mouse model with forebrain deletion of ankyrin-G, we found behavioral changes reminiscent of aspects of human bipolar disorder and synaptic and cellular changes correlating with the behavior changes, although we appreciate that translation from mouse model to human disease must be done with caution.

Some of previous attempts to develop genetic models of bipolar disorder in mice have used other loci, such as *CLOCK*, *DAT-1*, *NCAN*, or *SHANK3* (35–38). Many of these mouse models displayed behavioral hyperactivity or other features resembling patients with bipolar disorder. However, none of these genes (except *NCAN*) show genome-wide association with bipolar disorder. Furthermore, several of these mouse models have phenotypic limitations: *SHANK3*-overexpression mice had seizures and failed to respond to lithium, atypical for human bipolar disorder; the *Ncan* KO mice were not reported to have features related to depression (and there was no cellular and molecular characterization); *DAT-1* homozygous KO mice had decreased activity in response to methylphenidate; and heterozygous mice had mania-like behavior, but responsive predominantly to valproate, but less to lithium (39).

The previous study using viral vector-mediated knockdown of ankyrin-G in the hippocampus yielded intriguing behavioral changes, especially impulsive behaviors, with some increase in locomotor activity (20). However, compared with genetic models, viral injection has practical limitations. Genetic deletion of Ank3 exon 1b, a brain-specific isoform highly expressed in cerebellum (40) was also reported. Homozygous knockouts were ataxic, so heterozygotes were used for behavioral studies and showed relatively subtle changes with no locomotor hyperactivity. Thus, while this was a pioneering study, it did not provide a robust genetic model of bipolar disorder (20).

Our model involves substantial loss of ankyrin-G protein expression. By contrast, decreases of ankyrin-G in human postmortem brain in psychiatric disorders are relatively small (15). Moreover, mouse models of other neuropsychiatric disorders such as Huntington's disease or Parkinson's disease often use more severe genetic changes than seen in humans to achieve robust changes within the lifetime of mice (33), and our strategy is consistent with this experience.

Although the CaMKII-Cre driver expresses Cre at a relatively late developmental stage, we still found striking cellular and behavioral changes in Ank-G cKO mice. This suggests altered gene expression in adulthood can cause synaptic changes with consequent behavioral alterations and raises the possibility that some changes in human psychiatric disorders could also be due to synaptic changes in adulthood. The timing of the deletion of ankyrin-G may influence the nature of the behavioral phenotype. Schizophrenia has been more strongly related to developmental alterations than bipolar disorder (41). We might hypothesize that schizophrenia-like features would result from earlier loss of ankyrin-G expression in mice, while bipolar-like features might result from later loss of expression. A human patient with a deletion in ankyrin-G had a severe developmental phenotype with mental retardation (42), possibly reflecting change in expression in the entire brain throughout development.

At baseline, the Ank-G cKO mice exhibit striking hyperactivity, one of the core features of human mania, and a translatable phenotype which can be assessed in comparable ways in human patients and in mouse models (43–46). There was also increased exploratory behavior, decreased anxiety-like behavior, and decreased depression-like behavior, all comparable to behaviors characteristic of human mania. Patients with ADHD also have hyperactivity, paradoxically ameliorated by methylphenidate (30). By contrast, Ank-G cKO mice displayed increased activity with methylphenidate injection (at 10 or 30 mg/kg). The drug × gene × time interactions are significant, indicating cKO mice may bear different sensitivity to methylphenidate from control, although the key point is that there

were increases overall, not decreases. We did not detect severe deficits in cognitive tests, and cognition is generally reported to be more severely altered in schizophrenia than bipolar disorder (27, 47). Future studies could include more sensitive and sophisticated cognitive function tests. Sensory-motor gating as tested by PPI, strongly associated with schizophrenia but less consistently observed in bipolar patients (28, 48), was normal in cKO mice. There was dramatic response of key behaviors to lithium and VPA, the classic drugs for human mania. Thus, although it is important to be cautious when interpreting mouse behaviors in the context of human psychiatric disorders, especially given the overlap in etiology and phenotypes of bipolar disorder and schizophrenia (49), our results support the view that this mouse model displays a phenotype related more to bipolar disorder than to schizophrenia or ADHD.

Consistent with behavioral hyperactivity, there was increased c-fos, suggesting increased neuronal activity. Like the loss of ankyrin-G, the increase of c-fos label was present in pyramidal neurons, not interneurons. It is most likely that the neurons with increased c-fos are the same neurons with decreased Ank-G; however, we cannot exclude the possibility that circuit-based changes cause increased firing of a few remaining pyramidal neurons without loss of Ank-G to cause the behavioral hyperactivity. The brain regions with increased c-fos labeling correspond with changed functional activity: increased c-fos labeling in the motor and cingulate cortex could correlate, respectively, with elevated locomotor activity and altered emotion-related behavior.

The increased pyramidal cell activity likely reflects a combination of changes in intrinsic properties caused by changes in sodium/potassium channels at the AIS and circuit changes caused by loss of GABA inhibition at the AIS, presumably with the circuit changes predominating. There is loss of the GABA synthesizing enzyme GAD67 as well as the transporter GAT-1 in inhibitory presynaptic cartridge synapses. Thus, GABA signaling from chandelier synapses to the AIS is expected to be decreased. Disruption of local inhibitory cortical circuitry is emerging as a central mechanism for schizophrenia (50), with decreased cartridges on cortical pyramidal neurons in postmortem brain studies (18). Decreased inhibitory connections have also been reported for bipolar disorder (19). When quantifying cartridges, we chose piriform and cingulate cortex because unlike humans, who have clear cartridge synapses throughout the cortex, mice have the clearest and most distinctive cartridge synapses in piriform cortex, and to a lesser extent in cingulate cortex (26). Our findings are consistent with the concept of alterations of inhibitory synapses in bipolar disorder.

Multiple genetic risk factors including *ANK3* may converge into a few pathophysiological pathways in bipolar disorder, including GABA transmission (51). Recent findings implicate ankyrin-G in AMPA glutamate receptor–excitatory synapse structure and function, as well as in GABA synapses onto the cell body (12, 52). Future research may be designed to determine the contribution of these different aspects.

The Ank-G cKO mice do not undergo spontaneous cycling between mania-like and depression-like features. However, regular and spontaneous cycling is not a common phenotype in bipolar patients, who often have irregular episodes, including depression triggered by stress. The social defeat stress model is a well-accepted mouse model of human depression (32), and the Ank-G cKO mice showed increased susceptibility compared with controls. We thus suggest that our model represents a robust demonstration of both poles of behavior in a genetic mouse model of bipolar illness based on a gene with genome-wide significance in human genetic studies.

Nevertheless, there are limitations to our study. Mouse behavioral changes can only be imperfectly compared with human behavior. Most of the behavioral tests (except the 3D open field recording, which indicated even more robust changes in dark phases) were done only during day time. Studies were not powered to detect sex differences or sex × gene interactions. The human variation in ANK3 may also change splicing or regional brain expression in ways not modeled in the current study (7, 11, 13, 14, 53).

In conclusion, we found that Ank-G cKO mice displayed striking behavioral hyperactivity and alterations of emotion-related

NEUROSCIENCE

behaviors, with only mild changes in cognition, and no significant change in sensory-motor gating, suggesting a resemblance to human mania. The behavioral changes were substantially ameliorated by drugs specific for human mania. With social defeat stress, the mice switched to characteristic signs of depression-like behavior, and showed alternation between mania-like and depression-like behavior with repeated social defeat stress. Changes in GABA synapses may underlie some of the behavioral alterations and may represent synaptic plasticity during adulthood, contributing to the behavioral phenotypes. We propose these Ank-G cKO mice as a genetic mouse model of aspects of human bipolar affective disorder based on a locus with genome-wide significance for the human

disorder. The model may be useful for studying pathophysiology and for the development of experimental therapeutics.

1. Schizophrenia Working Group of the Psychiatric Genomics Consortium (2014) Biological insights from 108 schizophrenia-associated genetic loci. *Nature* 511:421–427.
2. Craddock N, Sklar P (2013) Genetics of bipolar disorder. *Lancet* 381:1654–1662.
3. Mühleisen TW, et al. (2014) Genome-wide association study reveals two new risk loci for bipolar disorder. *Nat Commun* 5:3339.
4. Chen DT, et al.; BiGS (2013) Genome-wide association study meta-analysis of European and Asian-ancestry samples identifies three novel loci associated with bipolar disorder. *Mol Psychiatry* 18:195–205, and erratum (2013) 18:264–266.
5. Ferreira MAR, et al.; Wellcome Trust Case Control Consortium (2008) Collaborative genome-wide association analysis supports a role for ANK3 and CACNA1C in bipolar disorder. *Nat Genet* 40:1056–1058.
6. Yuan A, et al. (2012) ANK3 as a risk gene for schizophrenia: New data in Han Chinese and meta analysis. *Am J Med Genet B Neuropsychiatr Genet* 159B:997–1005.
7. Roussos P, et al. (2012) Molecular and genetic evidence for abnormalities in the nodes of Ranvier in schizophrenia. *Arch Gen Psychiatry* 69:7–15.
8. Kordeli E, Lambert S, Bennett V (1995) AnkyrinG. A new ankyrin gene with neural-specific isoforms localized at the axonal initial segment and node of Ranvier. *J Biol Chem* 270:2352–2359.
9. Bender KJ, Trussell LO (2012) The physiology of the axon initial segment. *Annu Rev Neurosci* 35:249–265.
10. Jenkins PM, et al. (2015) Giant ankyrin-G: A critical innovation in vertebrate evolution of fast and integrated neuronal signaling. *Proc Natl Acad Sci USA* 112:957–964.
11. Nelson AD, Jenkins PM (2016) The splice is right: ANK3 and the control of cortical circuits. *Biol Psychiatry* 80:263–265.
12. Smith KR, et al. (2014) Psychiatric risk factor ANK3/ankyrin-G nanodomains regulate the structure and function of glutamatergic synapses. *Neuron* 84:399–415.
13. Quinn EM, et al. (2010) Evidence for cis-acting regulation of ANK3 and CACNA1C gene expression. *Bipolar Disord* 12:440–445.
14. Rueckert EH, et al. (2013) Cis-acting regulation of brain-specific ANK3 gene expression by a genetic variant associated with bipolar disorder. *Mol Psychiatry* 18:922–929.
15. Cruz DA, Weaver CL, Lovallo EM, Melchitzky DS, Lewis DA (2009) Selective alterations in postsynaptic markers of chandelier cell inputs to cortical pyramidal neurons in subjects with schizophrenia. *Neuropsychopharmacology* 34:2112–2124.
16. Howard A, Tamas G, Soltesz I (2005) Lighting the chandelier: New vistas for axo-axonic cells. *Trends Neurosci* 28:310–316.
17. Lewis DA, Sweet RA (2009) Schizophrenia from a neural circuitry perspective: Advancing toward rational pharmacological therapies. *J Clin Invest* 119:706–716.
18. Volk DW, Lewis DA (2002) Impaired prefrontal inhibition in schizophrenia: Relevance for cognitive dysfunction. *Physiol Behav* 77:501–505.
19. Guidotti A, et al. (2000) Decrease in reelin and glutamic acid decarboxylase67 (GAD67) expression in schizophrenia and bipolar disorder: A postmortem brain study. *Arch Gen Psychiatry* 57:1061–1069, and erratum (2002) 59:12.
20. Leussis MP, et al. (2013) The ANK3 bipolar disorder gene regulates psychiatric-related behaviors that are modulated by lithium and stress. *Biol Psychiatry* 73:683–690.
21. Jenkins PM, et al. (2013) E-cadherin polarity is determined by a multifunction motif mediating lateral membrane retention through ankyrin-G and apical-lateral transcytosis through clathrin. *J Biol Chem* 288:14018–14031.
22. O'Brien WT, et al. (2004) Glycogen synthase kinase-3beta haploinsufficiency mimics the behavioral and molecular effects of lithium. *J Neurosci* 24:6791–6798.
23. Golden SA, Covington HE, 3rd, Berton O, Russo SJ (2011) A standardized protocol for repeated social defeat stress in mice. *Nat Protoc* 6:1183–1191.
24. Hedstrom KL, et al. (2007) Neurofascin assembles a specialized extracellular matrix at the axon initial segment. *J Cell Biol* 178:875–886.
25. Wang X, Sun QQ (2012) Characterization of axo-axonic synapses in the piriform cortex of Mus musculus. *J Comp Neurol* 520:832–847.
26. Inda MC, DeFelipe J, Muñoz A (2009) Morphology and distribution of chandelier cell axon terminals in the mouse cerebral cortex and claustroamygdaloid complex. *Cereb Cortex* 19:41–54.
27. Bora E (2016) Differences in cognitive impairment between schizophrenia and bipolar disorder: Considering the role of heterogeneity. *Psychiatry Clin Neurosci* 70:424–433.
28. Kohl S, Heekeren K, Klosterkötter J, Kuhn J (2013) Prepulse inhibition in psychiatric disorders: Apart from schizophrenia. *J Psychiatr Res* 47:445–452.
29. Powell SB, Weber M, Geyer MA (2012) Genetic models of sensorimotor gating: Relevance to neuropsychiatric disorders. *Curr Top Behav Neurosci* 12:251–318.
30. Lakhan SE, Kirchgessner A (2012) Prescription stimulants in individuals with and without attention deficit hyperactivity disorder: Misuse, cognitive impact, and adverse effects. *Brain Behav* 2:661–677.
31. Lex C, Bäzner E, Meyer TD (2017) Does stress play a significant role in bipolar disorder? A meta-analysis. *J Affect Disord* 208:298–308.
32. Kudryavtseva NN, Bakshtanovskaya IV, Koryakina LA (1991) Social model of depression in mice of C57BL/6J strain. *Pharmacol Biochem Behav* 38:315–320.
33. Ross CA, Pletnikov MV (2013) Mouse models of schizophrenia and bipolar disorder. *Neurobiology of Mental Illness*, eds Charney DS, Buxbaum JD, Sklar P, Nestler EJ (Oxford Univ Press, Oxford), pp 287–300.
34. Logan RW, McClung CA (2016) Animal models of bipolar mania: The past, present and future. *Neuroscience* 321:163–188.
35. Han K, et al. (2013) SHANK3 overexpression causes manic-like behaviour with unique pharmacogenetic properties. *Nature* 503:72–77.
36. Miró X, et al. (2012) Studies in humans and mice implicate neurocan in the etiology of mania. *Am J Psychiatry* 169:982–990.
37. Roybal K, et al. (2007) Mania-like behavior induced by disruption of CLOCK. *Proc Natl Acad Sci USA* 104:6406–6411.
38. Zhuang X, et al. (2001) Hyperactivity and impaired response habituation in hyperdopaminergic mice. *Proc Natl Acad Sci USA* 98:1982–1987.
39. Ralph-Williams RJ, Paulus MP, Zhuang X, Hen R, Geyer MA (2003) Valproate attenuates hyperactive and perseverative behaviors in mutant mice with a dysregulated dopamine system. *Biol Psychiatry* 53:352–359.
40. Zhou D, et al. (1998) AnkyrinG is required for clustering of voltage-gated Na channels at axon initial segments and for normal action potential firing. *J Cell Biol* 143:1295–1304.
41. Owen MJ, O'Donovan MC, Thapar A, Craddock N (2011) Neurodevelopmental hypothesis of schizophrenia. *Br J Psychiatry* 198:173–175.
42. Iqbal Z, et al. (2013) Homozygous and heterozygous disruptions of ANK3: At the crossroads of neurodevelopmental and psychiatric disorders. *Hum Mol Genet* 22:1960–1970.
43. Cheniaux E, et al. (2014) Increased energy/activity, not mood changes, is the core feature of mania. *J Affect Disord* 152–154:256–261.
44. Henry BL, et al. (2010) Cross-species assessments of motor and exploratory behavior related to bipolar disorder. *Neurosci Biobehav Rev* 34:1296–1306.
45. Perry W, et al. (2010) Quantifying over-activity in bipolar and schizophrenia patients in a human open field paradigm. *Psychiatry Res* 178:84–91.
46. Scott J, et al. (2017) Activation in bipolar disorders: A systematic review. *JAMA Psychiatry* 74:189–196.
47. Burdick KE, et al. (2014) Empirical evidence for discrete neurocognitive subgroups in bipolar disorder: Clinical implications. *Psychol Med* 44:3083–3096.
48. Perry W, Minassian A, Feifel D, Braff DL (2001) Sensorimotor gating deficits in bipolar disorder patients with acute psychotic mania. *Biol Psychiatry* 50:418–424.
49. Potash JB, Bienvenu OJ (2009) Neuropsychiatric disorders: Shared genetics of bipolar disorder and schizophrenia. *Nat Rev Neurol* 5:299–300.
50. Lewis DA (2011) The chandelier neuron in schizophrenia. *Dev Neurobiol* 71:118–127.
51. Ament SA, et al.; Bipolar Genome Study (2015) Rare variants in neuronal excitability genes influence risk for bipolar disorder. *Proc Natl Acad Sci USA* 112:3576–3581.
52. Tseng WC, Jenkins PM, Tanaka M, Mooney R, Bennett V (2015) Giant ankyrin-G stabilizes somatodendritic GABAergic synapses through opposing endocytosis of GABAA receptors. *Proc Natl Acad Sci USA* 112:1214–1219.
53. Hughes T, et al. (2016) A loss-of-function variant in a minor isoform of ANK3 protects against bipolar disorder and schizophrenia. *Biol Psychiatry* 80:323–330.
54. Tsien JZ, et al. (1996) Subregion- and cell type-restricted gene knockout in mouse brain. *Cell* 87:1317–1326.
55. Madisen L, et al. (2010) A robust and high-throughput Cre reporting and characterization system for the whole mouse brain. *Nat Neurosci* 13:133–140.
56. Ayhan Y, et al. (2011) Differential effects of prenatal and postnatal expressions of mutant human DISC1 on neurobehavioral phenotypes in transgenic mice: Evidence for neurodevelopmental origin of major psychiatric disorders. *Mol Psychiatry* 16:293–306.
57. Pletnikov MV, et al. (2008) Inducible expression of mutant human DISC1 in mice is associated with brain and behavioral abnormalities reminiscent of schizophrenia. *Mol Psychiatry* 13:173–186, 115.
58. Chiu CT, Liu G, Leeds P, Chuang DM (2011) Combined treatment with the mood stabilizers lithium and valproate produces multiple beneficial effects in transgenic mouse models of Huntington's disease. *Neuropsychopharmacology* 36:2406–2421.
59. Gainetdinov RR, et al. (1999) Role of serotonin in the paradoxical calming effect of psychostimulants on hyperactivity. *Science* 283:397–401.
60. Kizhatil K, et al. (2007) Ankyrin-G and beta2-spectrin collaborate in biogenesis of lateral membrane of human bronchial epithelial cells. *J Biol Chem* 282:2029–2037.